Baryogenesis with relativistic bubble walls

Miguel Vanvlasselaer[a],[*]

[a]*Theoretische Natuurkunde and IIHE/ELEM, Vrije Universiteit Brussel, & The International Solvay Institutes, Pleinlaan 2, B-1050 Brussels, Belgium*

E-mail: *miguel.vanvlasselaer@vub.be

In this talk, we study the impact of first order phase transitions with fast bubble walls on mechanisms of leptogenesis and baryogenesis. We begin our exploration with the usual leptogenesis where the breaking of $B-L$ occurs via a PT with fast walls. Then we move to a more exotic case where the $B-L$ breaking phase transition creates heavy particles in the plasma and catalizes the leptogenesis. Finally, we apply the same production mechanism to the EWPT at low energy and build a new model of EWBG. Those models are all original and contain crucial new phenomenological aspects like the emission of large amount of Gravitational waves.

---

[*]Speaker

1. Introduction

One of the greatest puzzles of the early universe cosmology is the origin of the observed excess of matter over anti-matter, which is commonly parameterized by

$$Y_B \equiv \frac{n_B - n_{\bar{B}}}{s}\bigg|_0 = (8.75 \pm 0.23) \times 10^{-11} \tag{1}$$

with n_B, $n_{\bar{B}}$ and s respectively the number density of baryons, anti-baryons and the entropy density. The second equality comes from Planck data and evolution models of the early universe[1]. Within the inflationary paradigm, this asymmetry calls for an explanation in terms of early universe dynamics, a dynamics which is called *baryogenesis*. For a successful baryogenesis scenario, the well-known Sakharov requirements should be satisfied [2], namely the violation of the baryon number, violation of C and CP symmetries, and the presence of an out-of-equilibrium process. Many different mechanisms can fulfil those requirements, see [3, 4] for extensive reviews. On the top of this, baryogenesis mechanisms can be broadly classified into two different categories, depending of the SM sectors where the asymmetry originally forms: in the baryon sector, in the case of the original *baryogenesis scenario* or in the lepton sector, in the case of the so-called *leptogenesis scenario*[5].

First order phase transitions are very efficient ways to fulfil the out-of-equilibrium criterion, and it is used namely in the case of *electroweak baryogenesis* [6, 7]. Several BSM models could make the EWPT first order[8–12] (see [13] for review). However, relativistic bubble walls were believed to *suppress* the final baryon asymmetry[14–17].

In this paper we propose to reconsider this belief by discussing situations in which ultra-relativistic bubble walls actually can enhance the baryon/lepton asymmetry. We will discuss three different types of models taking advantage of fast walls: in section 3, we study the usual leptogenesis catalized by a phase transition (see also [18] for another viable model). The Right-Handed Neutrinos (RHN) abruptly receive a large mass upon crossing the bubble wall, and decay all together, suppressing the wash-outs.

In section 4, we study another model of leptogenesis catalized via the production of heavy states, which we identify with Majorana neutrinos. The idea is based on the observation in[19] that an ultra-relativistic bubble wall with Lorentz factor $\gamma_w \gg 1$, can produce in the plasma particles with mass up to $M \lesssim \sqrt{\gamma_w T_{\text{nuc}} \times v}$, where T_{nuc} and v are the nucleation temperature of FOPT and the scale of the symmetry breaking respectively. Beside being an out-of-equilibrium production channel, we will also show that this production mechanism can be naturally CP-violating. We confirm the statements above by analyzing the CP-violating effects in the interference of tree and one loop level processes.

Finally, in section 5, we study a model for which the Electroweak phase transition, again with fast bubbel walls, produces heavy states and catalizes EWBG.

One of the interesting feature of the class of models we discuss in this paper is that it requires ultra-relativistic bubble wall velocities and strong phase transition, and then is generically accompanied with strong gravitational waves signal.

2. When do the walls become fast? (and how fast ?)

For strong first order phase transitions, with moderate to strong supercooling, which will be the natural territory of exploration of this paper, the regime of expansion of the bubble walls can be determined by the balance between the driving force and the plasma pressure

$$\Delta V = \Delta \mathcal{P}(\gamma_w = \gamma_w^{\text{ter}}), \tag{2}$$

where γ_w^{ter} is the terminal velocity of the bubble. If this equality is never fulfilled, we expect the wall to runaway and to keep accelerating until the bubble collisions(see however [20, 21]).

In general, $\Delta \mathcal{P}(\gamma_w)$ is expected to be a very complicated function of the velocity γ_w, however, it simplifies in the regime of large $\gamma_w \gg 1$ to a sum of few contributions. The leading order pressure due to particles gaining a mass is given by [22]

$$\mathcal{P}_{\text{BM}} \equiv \frac{1}{48} \sum_i g_i n_i \Delta M_i^2 T^2, \tag{3}$$

where particle i has g_i degrees of freedom, and $n_i = 1(2)$ for fermions (bosons), while emission of soft gauge bosons leads to a $\gamma_w v T^3 \log(v/T)$ term[23–25]. Using the results presented in [24, 25], we can obtain the terminal velocity for large supercoolings:

$$\gamma^{\text{ter}} \sim 6 \times \left(\frac{\Delta V - \Delta \mathcal{P}_{\text{LO}}^{SM}}{(100 \text{ GeV})^4} \right) \left(\frac{100 \text{GeV}}{T_{\text{nuc}}} \right)^3 \frac{1}{\log \frac{M_z}{gT}}. \tag{4}$$
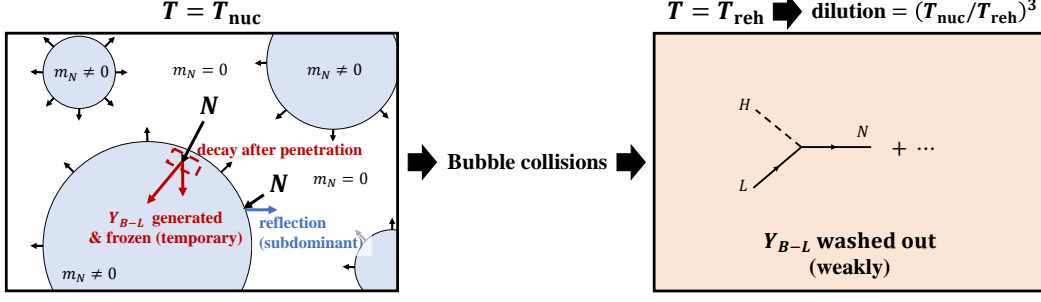
3. Bubble-assisted leptogenesis

We start our exploration of the effect of fast walls on lepton and baryon yields with the simplest leptogenesis-like case[26]. The setup we consider is as follows: The RHNs receive a large Majorana mass via the spontaneous symmetry breaking of $B - L$, which is first order and proceeds via the nucleation of bubbles (see Ref. [17] for the study of the second-order case). The relevant part of the Lagrangian can be written in the mass basis of the RHNs as

$$\mathcal{L}_{\text{int}} = \frac{1}{2} \sum_I y_I \Phi \bar{N}_I^c N_I + \sum_{\alpha, I} Y_{D,\alpha I} H \bar{L}_\alpha N_I + h.c., \tag{5}$$

where L_α are the SM lepton doublets, N_I are the three families of heavy right-handed neutrinos, $Y_{D,\alpha I}$ are the *Dirac* Yukawa couplings between N_I and L_α, and y_I are *Majorana* Yukawa couplings. After the phase transition, $\langle \Phi \rangle \equiv v_\phi/\sqrt{2}$, and the type-I seesaw Lagrangian is recovered with $M_I = \frac{1}{\sqrt{2}} y_I v_\phi$.

In the thermal leptogenesis scenario, the expansion of the universe fulfils the out-of-equilibrium Sakharov criterion. It is however typically a quite weak departure from equilibrium and the efficiency of traditional thermal leptogenesis is suppressed by the fact that most of heavy neutrinos decay *in equilibrium*. This suppression is usually parameterized by a $\kappa_{\text{wash}} \sim 0.01$ which gives the final baryon asymmetry

$$Y_B = Y_N^{\text{eq}} \epsilon_{\text{CP}} \kappa_{\text{sph}} \kappa_{\text{wash}}. \tag{6}$$

Figure 1: Schematic picture of the bubble-assisted leptogenesis scenario during bubble expansion (left) and after bubble collisions (right).

where $Y_N^{\rm eq}$ is the initial abundance of RHNs, $\epsilon_{\rm CP} \lesssim 0.1$ is the parameter controlling the CP violation during decay and the factor $\kappa_{\rm sph} \sim 1/3$ designates the conversion from the lepton asymmetry into a baryon asymmetry.

In the case of *bubble-assisted* leptogenesis[26], the RHNs are massless outside the FOPT bubbles and become suddenly massive when the wall hits them. a cartoon of the situation is provided in Fig.1. The expansion of the bubble wall actually offers a new source of departure from equilibrium and opens the possibility to drastically enhance $\kappa_{\rm wash} \to 1$. This is because if the RHNs become suddenly massive, they *all* decay out-of-equilibrium, not only a $\mathcal{O}(0.01)$ fraction of it (when the inverse decays are alreade decoupled).

However, new possible sources of suppression come in compensation: i) first the RHNs might fail to enter the bubble and be reflected away, this is encapsulated by $\kappa_{\rm pen}$, ii) our setup opens new channels like $N_I N_I \to \phi\phi$, where the number density of RHN is depleted before its decay, therefore suppressing the final asymmetry and that we designates by $\kappa_{\rm dep}$, iii) at the end of the PT, entropy is injected in the plasma and dilutes any previous abundances by a factor $(T_{\rm nuc}/T_{\rm reh})^3$. At the end, the asymmetry is parameterized by

$$Y_B = Y_N^{\rm eq} \epsilon_{\rm CP}\, \kappa_{\rm sph}\, \kappa_{\rm pen}\, \kappa_{\rm dep}\, \kappa_{\rm wash} \left(\frac{T_{\rm nuc}}{T_{\rm reh}}\right)^3, \tag{7}$$

where $Y_N^{\rm eq}$ is population of RHNs outside the bubbles. $T_{\rm reh}$ is the temperature after the FOPT and can be estimated via

$$\left(\frac{T_{\rm nuc}}{T_{\rm reh}}\right)^3 \simeq (1 + \alpha_n)^{-3/4}. \tag{8}$$

Our goal is to determine the values of each parameter $Y_N^{\rm eq}, \epsilon_{\rm CP}, \kappa_{\rm sph}, \kappa_{\rm pen}, \kappa_{\rm dep}, \kappa_{\rm wash}, \left(\frac{T_{\rm nuc}}{T_{\rm reh}}\right)^3$ as a function of the PT parameters α_n and β. The $\kappa_{\rm pen}$ parameter can be obtained by computing the terminal velocity of the bubble wall, via the methods discussed in Section 2 and using the fact that a RHN will enter the wall if its momentum all the direction of the wall expansion (in the wall frame) $p_z^{\rm wf}$ is larger than its mass inside the wall M_I: $p_z^{\rm wf} > M_I$. Integrating over the density of incoming RHN impinging the wall gives the fraction of entering RHN.

Computing κ_{dep} and κ_{wash} requires to solve the relevant Boltzmann equations. We first assume that the RHN are in kinetic equilibrium with the SM thermal bath *also inside the bubble*, due to the efficient interaction $\phi N \to \phi N$ via N mediation. This allows to integrate the Boltzmann equations over the momenta. The Boltzmann equation in this procedure become

$$\dot{n}_{N_I} + 3Hn_{N_I} = -\sum_{A,B}\left(2\langle\sigma v\rangle_{N_I N_I \to AB}\, n_{N_I}^2 - 2\langle\sigma v\rangle_{AB \to N_I N_I}\, n_A n_B\right) - \Gamma_D(N_I)n_{N_I}, \quad (9)$$

$$\dot{n}_{B-L} + 3Hn_{B-L} = -\sum_I \epsilon_I \Gamma_D(N_I)n_{N_I} + (\text{wash-out}), \quad (10)$$

where $\Gamma_D(N_I)$ is the total decay rate of N_I and ϵ_I is the CP-violating parameter for N_I defined by

$$\epsilon_I \equiv \frac{\Gamma(N_I \to HL) - \Gamma(N_I \to \bar{H}\bar{L})}{\Gamma(N_I \to HL) + \Gamma(N_I \to \bar{H}\bar{L})}, \quad (11)$$

where $\bar{L}$ denotes the anti-particle of L. The initial population of N_I within the bubbles will be given by its massless equilibrium distribution scaled by a factor of κ_{pen}:

$$n_{N_I}^{(0)} = \kappa_{\text{pen}} \frac{2 \cdot \frac{3}{4} \cdot \zeta(3)}{\pi^2} T_{\text{nuc}}^3. \quad (12)$$

We have also checked that that the RHNs decay before the onset of bubble collisions. the depletion can decrease the initial abundance of N_I via $N_I N_I \to \phi\phi$, or directly $N_I N_I \to f\bar{f}$, with f being a SM fermion, in the case in which $B - L$ is gauged. Finally, the flavor changing interactins $N_I N_I \leftrightarrow N_J N_J$ are also efficient and maintain equilibrium among the RHN flavors.

This allows to define $n_N \equiv \sum_I n_{N_I} \simeq 3n_{N_1} \simeq 3n_{N_2} \simeq 3n_{N_3}$ and $Y_N \equiv n_N/s$, we obtain the familiar looking equations

$$zHs\, Y_N'(z) = -\bar{\gamma}_D\left(\frac{Y_N}{Y_N^{(\text{eq})}} - 1\right) - 2\gamma_{NN \to \phi\phi}\left(Y_N^2 - \left(Y_N^{(\text{eq})}\right)^2\right) + (\text{model-dependent}), \quad (13)$$

$$zHs\, Y_{B-L}'(z) = -\epsilon_{\text{CP}}\bar{\gamma}_D\left(\frac{Y_N}{Y_N^{(\text{eq})}} - 1\right) - \frac{1}{2}(c_L + c_H)\,\bar{\gamma}_D \frac{Y_{B-L}}{Y^{(\text{eq})}}, \quad (14)$$

where $z \equiv M_N/T$, $Y_N^{(\text{eq})} = n_N^{(\text{eq})}/(\frac{2\pi^2}{45}g_* T^3)$ with the equilibrium number density $n_N^{(\text{eq})}$, $Y_N^{(\text{eq})} = (\frac{2}{\pi^2}T^3)/(\frac{2\pi^2}{45}g_* T^3)$, and

$$\bar{\gamma}_D \equiv \sum_I \gamma_D(N_I) = \sum_I n_{N_I}^{(\text{eq})} \frac{K_1(z)}{K_2(z)}\Gamma_D(N_I), \quad (15)$$

$$\epsilon_{\text{CP}}\,\bar{\gamma}_D \equiv \sum_I \epsilon_I \gamma_D(N_I), \quad (16)$$

$$\gamma_{NN \to \phi\phi} \equiv \frac{1}{9}s^2 \sum \langle\sigma v\rangle_{N_I N_I \to \phi\phi}. \quad (17)$$

This procedure permits to obtain a value for κ_{dep}. Finally κ_{wash} can be obtained by solving the Boltzmann equations in a way similar to the usual thermal leptogenesis, but using the reheating temperature T_{reh} as an initial temperature. Iterating this procedure over α_n and β, we obtain the
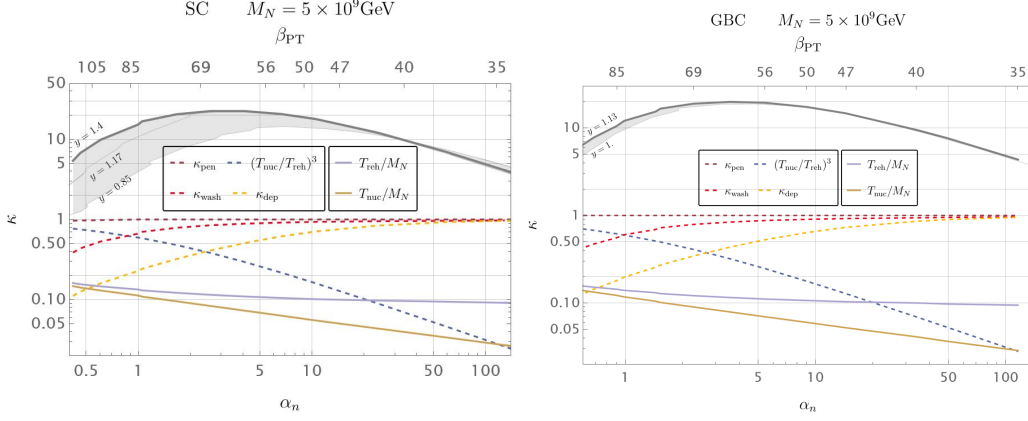
Figure 2: Comparison of the thermal leptogenesis and the bubble-assisted leptogenesis when the PT is catalized by a singlet (Left) or gauge bosons (Right).

plots in Fig. 2, in the case $M_N = 5 \times 10^9$ GeV. For the PT sector, we consider either that the phase transition is catalized by a singlet scalar (left panel) coupling only to Φ or that $B - L$ is gauged and that the PT is catalized by the $B - L$ gauge bosons (right panel). The two results mostly differ because of the different depletion channels existing in those two scenario. The grey bands show the amount of enhancement we obtain compared to the conventional thermal leptogenesis, and the horizontal axis shows the strength of the supercooling, α_n. We obtain a $O(20)$ enhancement compared to the thermal scenarios.

The fraction of RHNs entering into the bubble, κ_{pen} is order one in the whole parameter space, but slightly decreases when $\alpha_n \sim 1$. On the other hand, for stronger phase transition and thus more drastic departure from equilibrium $\alpha_n > 5$, $\kappa_{\text{wash}} \simeq 1$. In this regime, the washout suppression inherent to thermal leptogenesis is avoided. We find that κ_{dep} causes a stronger suppression compared to κ_{wash}, highlighting the importance of including these new annihilation channels, but it also becomes suppressed for larger α_n. However, even if, at large values of α_n, the washout and depletion effects become negligible, the dilution factor due to entropy injection, $(T_{\text{nuc}}/T_{\text{reh}})^3 = (1 + \alpha_n)^{-3/4}$ strongly suppress the baryon yield. The final asymmetry is proportional to the all these factors and we find the enhancement is maximized around $\alpha_n \sim 5$ and $\beta \sim 60$.

We emphasize that such strong and slow FOPT would produce copious background of GW, that might be detectable at the ET observer for the model presented above.

4. Leptogenesis via the production of heavy states

In the former scenario, bubbles were critical for giving a sudden large mass to the RHN and thus suppressing the wash-outs due to inverse decays. The main novelty with respect to thermal leptogenesis was that the RHN received a Majorana mass from a FOPT. We now turn to more exotic mechanism where the bubble walls create very heavy states from the light states of in plasma[19].

4.1 Production of heavy states with a fast bubbel wall

We start by reviewing the process of heavy states production from fast expanding bubbles presented in[19]. Let us assume the following Lagrangian

$$\mathcal{L} = |\partial_\mu \Phi|^2 + i\bar{\chi}\slashed{\partial}\chi + i\bar{N}\slashed{\partial}N - M_N\bar{N}N - Y\Phi\bar{N}\chi \tag{18}$$

where χ a light fermion and N a heavy Dirac fermion with mass $M_N \gg \langle\Phi\rangle$, $M_N \gg T_{\text{nuc}}$ and Y is the coupling between the scalar and the two fermions. We work in the basis where fermion masses are real. In this setting, the equilibrium abundance of N is exponentially suppressed. However in the case of an ultra-relativistic bubble expansion, the probability that the light χ fluctuates via mixing to the heavy N is non-vanishing [19] and is approximately equal to

$$\mathcal{P}^{\text{tree}}(\chi \to N) \approx \frac{Y^2\langle\Phi\rangle^2}{M_N^2}\Theta(\gamma_w T_{\text{nuc}} - M_N^2 L_w) \tag{19}$$

with $L_w \sim 1/m_\Phi$ the thickness of the wall. Thus, when the ultra-relativistic wall hits the plasma, it produces N and N^c. Note that this abundance will be much larger than its equilibrium value. Indeed, outside of the bubble we have

$$n_{N_I}^{\langle\Phi\rangle=0}(T_{\text{nuc}}) \simeq 0, \quad \text{Heavy } N_I \text{ have decayed} \tag{20}$$

while inside it became

$$\begin{aligned}
n_{N_I}^{\langle\Phi\rangle\neq0} &\simeq \frac{1}{\gamma_w v_w}\int \frac{d^3p}{(2\pi)^3}P_{\chi\to N}(p) \times f_\chi(p, T_{\text{nuc}}) \\
&\simeq \sum_i \frac{|Y_{iI}|^2\langle\Phi\rangle^2}{M_I^2\gamma_w v_w}\int \frac{d^3p}{(2\pi)^3} \times f_\chi^{eq}(p, T_{\text{nuc}})\Theta(p_z - M_I^2/\langle\Phi\rangle) \\
&\simeq \sum_i \theta_{iI}^2 n_{\chi^i}^{\langle\phi\rangle=0}(T_{\text{nuc}}).
\end{aligned} \tag{21}$$

where we used all through the computation $v_w = \sqrt{1 - 1/\gamma_w^2} \approx 1 - \frac{1}{2\gamma_w^2}$ is the velocity of the wall. We have defined the effective *mixing angle*

$$\theta_{iI} \equiv \frac{|Y_{iI}|\langle\Phi\rangle}{M_I}. \tag{22}$$

We now need to show that, at one loop level, interference within the bubble wall can create a difference abundance of N and N^c.

4.2 CP violation in production

To introduce CP violation in our production process, we will need to generalise the former Lagrangian of Eq. (18) to include several families of light species χ and heavy species N,

$$\mathcal{L} = i\bar{\chi}_i P_R\slashed{\partial}\chi_i + i\bar{N}_I\slashed{\partial}N_I - M_I\bar{N}_I N_I - Y_{iI}\phi\bar{N}_I P_R\chi_i - y_{I\alpha}(H\bar{L}_\alpha)P_R N_I + h.c, \tag{23}$$

where H and L_α have already been defined in section 3, P_R, P_L are the chiral projectors, that we now make explicit. We choose this assignment of chirality in agreement with our further toy models. Notice the difference with the Lagrangian in (5) where Φ was giving a mass to the RHN, while here we assume that another mechanism provides a mass to the RHN. In this sense, the transition of the Φ in the present scenario occurs *after* the usual leptogenesis from the decay of heavy N.
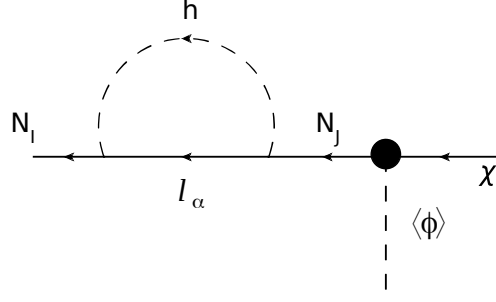
Figure 3: The diagram contributing to the function $f^{(HL)}$.

4.2.1 Calculation of the light → heavy transition *at 1-loop level*

Let us now compute the asymmetries in the populations of the various particle immediately after the PT in the case of the model in Eq.(23).

We first notice that, for the same reason than in usual out-of-equilibrium decay, CP violation cannot appear at tree level since processes will be proportional to $|Y_{iI}|^2$. As a consequence, we need to consider one loop corrections to it. To simplify the computations, we specialize to the case of ultra-relativistic bubble walls. First of all we need to know the CP violating effects in the $\chi_i \rightarrow N_I$ transition. Such effects appear due to the interference between tree-level and loop level diagram and scale like

$$
\begin{aligned}
A(\chi_i \rightarrow N_I)_{\text{tree}} &\propto Y_{iI} \\
A(\chi_i \rightarrow N_I)_{1-\text{loop}} &\propto \sum_{k,J} Y_{iJ} Y_{kJ}^* Y_{kI} \times f_{IJ}^{(\chi\phi)} + \sum_{\alpha,J} Y_{iJ} y_{\alpha J}^* y_{\alpha I} \times f_{IJ}^{(HL)}
\end{aligned}
\tag{24}
$$

where the functions $f^{(HL)}$ and $f^{(\chi\phi)}$ refer to the loop diagrams with virtual χ, ϕ and HL respectively. The computation of the loop shown in Fig.(3) in the background of the bubble wall gives

$$
\epsilon_{Ii} \equiv \frac{|\mathcal{M}_{i \rightarrow I}|^2 - |\mathcal{M}_{\bar{i} \rightarrow \bar{I}}|^2}{\sum_i |\mathcal{M}_{i \rightarrow I}|^2 + |\mathcal{M}_{\bar{i} \rightarrow \bar{I}}|^2}
\tag{25}
$$

$$
= \frac{2 \sum_{k,J} \text{Im}(Y_{iI} Y_{iJ}^* Y_{kJ} Y_{kI}^*) \text{Im} f_{IJ}^{(\chi\phi)}}{\sum_i |Y_{iI}|^2} + \frac{2 \sum_{\alpha,J} \text{Im}(Y_{iI} Y_{iJ}^* y_{\alpha J} y_{\alpha I}^*) \text{Im} f_{IJ}^{(HL)}}{\sum_i |Y_{iI}|^2},
\tag{26}
$$

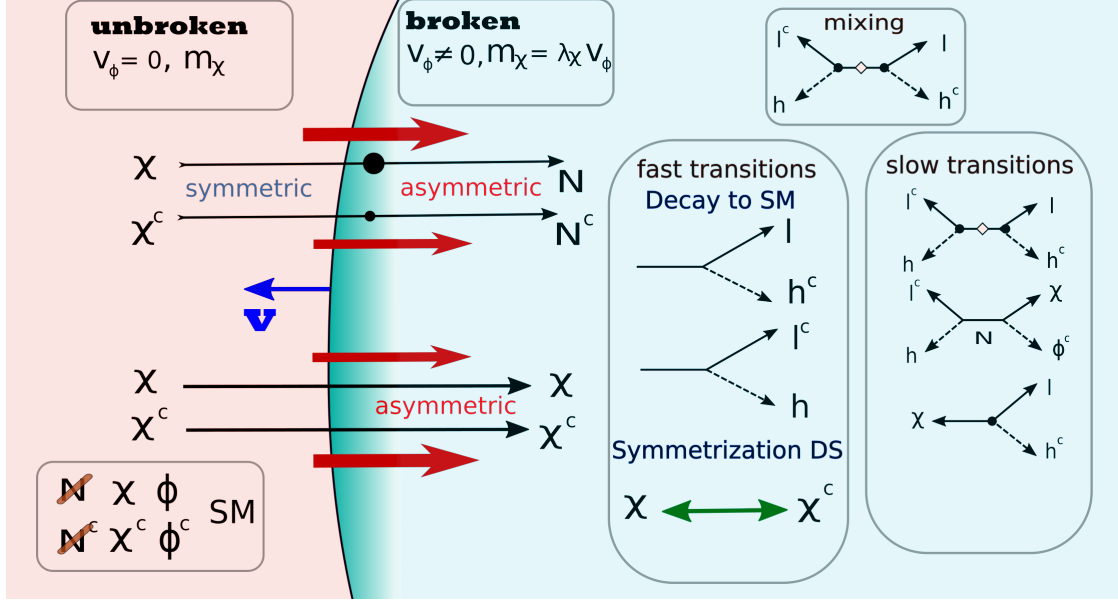where the loop functions take a form reminiscent from the out-of-equilibrium decay ones:

$$
\text{Im}[f_{IJ}^{(HL)}(x)] = \frac{1}{16\pi} \frac{\sqrt{x}}{1-x}, \qquad x = \frac{M_J^2}{M_I^2}
\tag{27}
$$

$$
\text{Im}[f_{IJ}^{(\chi\phi)}(x)] = \frac{1}{32\pi} \frac{1}{1-x}.
\tag{28}
$$

Summing over the flavours of χ_i we arrive at the following asymmetry in N_I abundance

$$
\epsilon_I \equiv \sum_i \epsilon_{Ii} = \frac{2 \sum_{\alpha,J,i} \text{Im}(Y_{iI} Y_{iJ}^* y_{\alpha J} y_{\alpha I}^*) \text{Im} f_{IJ}^{(HL)}}{\sum_i |Y_{iI}|^2}.
\tag{29}
$$

Figure 4: Mechanism at play in the phase transition-induced leptogenesis. Picture from [27].

We notice that the contribution from the χ, ϕ loop vanished after summing over the contributions. This shows that the passage of the bubble wall can create a difference in the abundances of N_I and $\bar{N}_I$ inside the bubble.

However since the N_I are produced by $1 \to 1$ transitions (conserving the total number of particles) the same difference will be present inside the bubble also for the abundances of $\bar{\chi}_i$ and χ_i, which means that some of the abundance of χ_i has been removed from the plasma:

$$\sum_I \Delta n_{N^I} = -\sum_i \Delta n_{\chi^i} \Rightarrow \qquad \sum_I \left(\Delta n_{N^I} - \Delta n_{\bar{N}^I}\right) = -\sum_i \left(\Delta n_{\chi^i} - \Delta n_{\bar{\chi}^i}\right), \qquad (30)$$

where $\Delta n_{N,\chi}$ are the differences in abundances of the particles in the broken and unbroken phases. The passage of the wall still did not create L number but separated it in a heavy and a light sector.

We can now move to the full model of leptogenesis with a fast bubble wall. Let us consider the following extension of the Lagrangian in Eq.23, where we have introduced Φ-dependent Majorana mass for the field χ and kept the rest of the interactions the same. Interestingly, only one specie of the Majorana fermion χ is sufficient for the generation of CP phase:

$$\mathcal{L}_{\text{int}} = \underbrace{\sum_I \left(Y_I (\phi^\dagger \bar{\chi}) P_L N_I + Y_I^\star \bar{N}_I P_R (\phi \chi) \right) - V(\phi) + \frac{1}{2} \lambda_\chi \phi \bar{\chi}^c \chi + \sum_I M_I \bar{N}_I N_I}_{\text{Toy model of Dark Sector}} \qquad (31)$$

$$+ \underbrace{\sum_{\alpha I} y_{\alpha I} (h \bar{l}_{\alpha, SM}) P_R N_I + h.c.,}_{\text{Connection to SM}}$$

We give the following $U(1)$ assignments, $L(\chi) = -1$, $L(N) = 1$ and $L(\phi) = 2$, which respect $U(1)$ lepton number. This $U(1)$ symmetry is obviously broken after the phase transition. The generation

Baryogenesis with relativistic bubble walls Miguel Vanvlasselaer

of the baryon asymmetry is illustrated in Fig.4 and proceeds as follows: The expansion of the bubble generates an asymmetry in N and χ, with an opposite sign. Immediately after the transition, the asymmetry in χ is washed out due to the lepton-number violating Majorana mass term. The asymmetry is then transmitted to the SM when the N decay via $N \to HL$, and produce

$$
\begin{aligned}
\frac{n_L - n_{L^c}}{s} &\simeq \frac{1}{s(T_{\text{reh}})} \sum_{iI} \epsilon_{Ii} \frac{3\zeta(3)|Y_{iI}|^2 T_{\text{nuc}}^3 \langle\phi\rangle^2}{4\pi^2 M_I^2} \times \frac{Br(N_I \to HL)}{Br(N_I \to HL) + Br(N_I \to \chi\Phi)} \\
&\simeq \frac{135\zeta(3)g_\chi}{8\pi^4 g_\star} \left(\frac{T_{\text{nuc}}}{T_{\text{reh}}}\right)^3 \sum_I \theta_I^2 \frac{2\sum_{\alpha,J} \text{Im}(Y_I Y_J^* y_{\alpha J} y_{\alpha I}^*)\text{Im}f_{IJ}^{(HL)}}{|Y_I|^2} \frac{\sum_\alpha |y_{\alpha I}|^2}{\sum_\alpha |y_{\alpha I}|^2 + |Y_I|^2},
\end{aligned}
\tag{32}
$$

where g_* is total number of degrees of freedom and $s(T) = \frac{2\pi^2}{45} g_\star T^3$, and g_χ is the number of degrees of freedom of χ particle. On the top of the CP violation in the N production, there is also a CP violation in the decay of N,

$$
\frac{n_L - n_{L^c}}{s}\bigg|_{\text{decay}} \sim \sum_I \frac{\theta_I^2}{g_\star} \epsilon_{\text{decay}}^I \left(\frac{T_{\text{nuc}}}{T_{\text{reh}}}\right)^3 \times \frac{\sum_\alpha |y_{\alpha I}|^2}{\sum_\alpha |y_{\alpha I}|^2 + |Y_I|^2}.
\tag{33}
$$

This constitutes a second source of asymmetry for the system, via the usual CP-violating decay. We will see that the dominant contribution depends on the different couplings of the systems. This asymmetry in return is passed to the baryons by sphalerons, similarly to the original leptogenesis models [28]. And adding the contribution from the production and from the decay, we obtain

$$
\begin{aligned}
\frac{\Delta n_B}{s} \equiv \frac{n_B - n_{\bar{B}}}{s} \simeq \quad & -\frac{28}{79} \times \frac{135\zeta(3)g_\chi}{8\pi^4 g_*} \times \sum_I \theta_I^2 \sum_{\alpha,J} \text{Im}(Y_I Y_J^* y_{\alpha J} y_{\alpha I}^*)\text{Im}f_{IJ}^{(HL)} \\
& \times \left(\frac{2}{|Y_I|^2} - \frac{1}{\sum_\alpha |y_{\alpha I}|^2}\right) \left(\frac{T_{\text{nuc}}}{T_{\text{reh}}}\right)^3 \frac{\sum_\alpha |y_{\alpha I}|^2}{\sum_\alpha |y_{\alpha I}|^2 + |Y_I|^2}.
\end{aligned}
\tag{34}
$$

The prefactor $-\frac{28}{79}$ comes from the sphalerons rates (see [29]). By assuming $O(1)$ parameters in the potential and dominant latent heat, $T_{\text{reh}} \sim v$. The factor $\frac{\sum_\alpha |y_{\alpha I}|^2}{\sum_\alpha |y_{\alpha I}|^2 + |Y_I|^2}$ appears since a part of the asymmetry in N is decaying back to $\phi\chi$.

Let us examine various bounds on the construction proposed. The non-vanishing VEV in the Lagrangian (31) generates a dimension 5 Weinberg operator of the see-saw form [30–34]

$$
O_W = \sum_{I,\alpha,\beta} \theta_I^2 \frac{y_{\alpha I} y_{\beta I}^* (\bar{L}_\alpha^c H)(L_\beta H)}{m_\chi}
\tag{35}
$$

which induces a mass for the heaviest light neutrinos

$$
\Rightarrow \text{Max}[m_\nu] \sim \text{Max}\left[\sum_I |y_{\alpha I}|^2 \theta_I^2\right] \frac{v_{EW}^2}{m_\chi}.
\tag{36}
$$

Combining Eqs. (34), (36) with observed neutrino mass scale and the constraints $\text{Max}[\theta_I^2] \gtrsim 10^{-5}$, $y \sim O(1)$, we obtain the following constraints

$$
\Rightarrow \quad m_\chi \gtrsim 5 \times 10^9 \text{GeV} \quad \Rightarrow \quad \langle\Phi\rangle \gtrsim 10^9 \text{GeV}.
\tag{37}
$$

PoS(CORFU2023)049

The inverse decay due to collisions $HL \to N$ will efficiently erase the asymmetry. The Boltzmann equation controlling this wash out is

$$\frac{dY_{\Delta_\alpha}}{dz} \simeq -\frac{0.42 e^{-z} z^{5/2}}{g_*^{1/2} g_\alpha} \left(\frac{M_P}{m_\chi}\right) \left(\frac{g_\chi \Gamma_\alpha}{m_\chi}\right) Y_{\Delta_\alpha}, \qquad \Gamma_\alpha \approx \left|\sum_I y_{\alpha I} \theta_I\right|^2 \frac{m_\chi}{8\pi g_\chi}. \tag{38}$$

from which we obtain that Y_{Δ_α} remains invariant for $m_\chi/T_{\text{reh}} \gtrsim 15$ (for the scale $m_\chi \sim 10^9$ GeV). The following approximate relation for the minimal m_χ/T_{reh} to avoid wash out is valid

$$\frac{m_\chi}{T_{\text{reh}}} \gtrsim \log \frac{M_P}{m_\chi} - 9 \tag{39}$$

where we took $\theta_I \sim 10^{-2}$ as a typical value. The $\Delta L = 2$ lepton violating operator $LLHH$, if it enters in equilibrium will also erase the initial asymmetry

$$\Gamma(H^c L_\alpha \to HL_\beta^c)(T) \approx \frac{4}{1.2\pi^2 g_\alpha} \sum_{iI} \frac{\theta_{iI}^4}{m_\chi^2} y_{i\alpha}^2 y_{i\beta}^2 T^3 \approx \frac{2}{1.2\pi^2} \left(\frac{m_\nu}{v_{EW}^2}\right)^2 T^3,$$

$$\Rightarrow T_{\text{reh}} \lesssim 5\sqrt{g_\star} \frac{v_{EW}^4}{M_P m_\nu^2} \sim 5 \times 10^{12} \text{ GeV}, \tag{40}$$

where we took $m_\nu^2 \sim 0.0025$ eV^2.

In conclusion we can see that this construction can lead to a viable mechanism of leptogenesis if there is a mild hierarchy between the scales; $M_I > \langle\Phi\rangle$ and $m_\chi, M_I > T_{\text{reh}}$. Finally, we obtain that the matching with the light neutrino masses makes this mechanism operative in the range of scales 10^9 GeV $< \langle\Phi\rangle < 5 \times 10^{12}$ GeV.

5. EW baryogenesis via PT with fast bubble walls

In the previous sections, we have discussed the high energy leptogenesis catalyzed by the passage of a fast bubble wall. ElectroWeak baryogenesis also relies on the out-of-equilibrium situation surrounding the bubble wall, but it is efficient *only if the velocity of the bubble wall is not much faster than the sound speed*[36]. On the other hand, gravitational wave amplitude is typically maximized for large velocities $v_w \to 1$[37], which makes large GW signal and efficient baryogenesis more or less mutually exclusive.

However in this section, we would like to use the mechanism proposed above, using large velocities and thus predicting copious amount of GW, to build a model of EWBG. One robust prediction of such a scenario is the large amount of GW emitted at the transition, with peak frequency fixed by the scale of the transition $f_{\text{peak}} \sim 10^{-3} \frac{T_{\text{reh}}}{\text{GeV}}$ mHz (see [38] for review). Such SGWB signal could be detected in future GW detectors such as LISA[37, 39], eLISA[40], LIGO[41, 42], BBO[43, 44], DECIGO[45–47], ET[48–50], AION[51], AEDGE[52]. This array of observers will be able to probe GW with frequencies in the window of mHz to kHz, which is the optimal scale for this mechanism to take place.
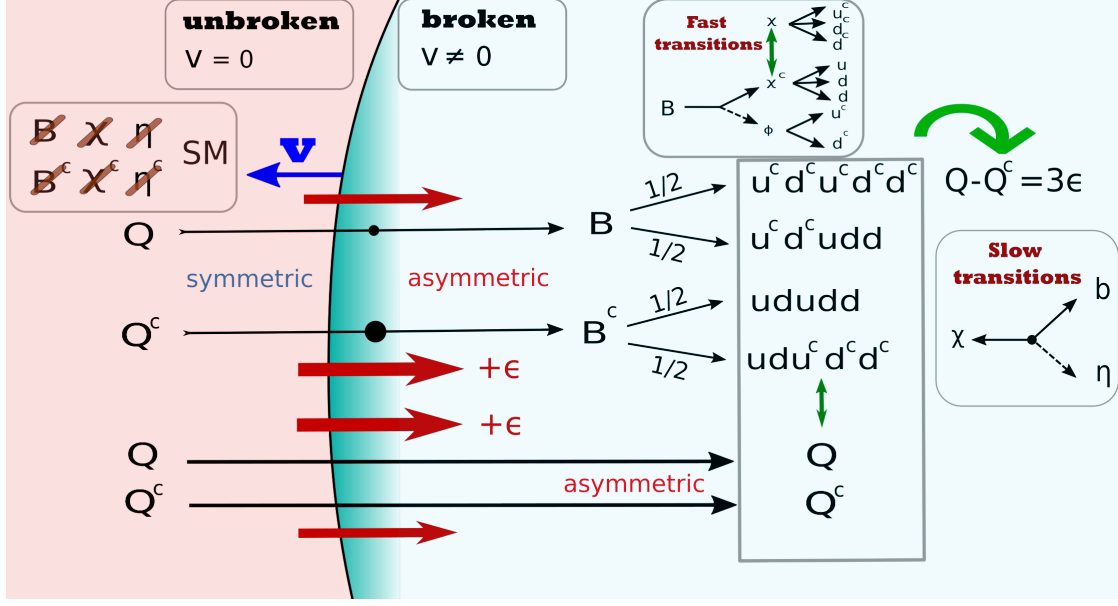
Figure 5: Mechanism at play in the low energy baryogenesis, from [35].

Below we present a prototype model, which we can consider as a first simple toy model:

$$\mathcal{L} = \quad \mathcal{L}_{SM} + m_\eta^2 |\eta|^2 + \sum_{I=1,2} M_I \bar{B}_I B_I$$

$$+ \quad \left(\sum_{I=1,2} Y_I (\bar{B}_I H) P_L Q + y_I \eta^* \bar{B}_I P_R \chi + \kappa \eta^c du + \frac{1}{2} m_\chi \bar{\chi}^c \chi + h.c. \right). \tag{41}$$

The model contains a Majorana field χ and two vector-like B quarks with the masses $M_{1,2} \sim m_\chi$. η is a scalar field (a diquark) which is in the fundamental representation of QCD with electric charge $Q(\eta) = 1/3$, Q, u, d are the SM quark doublet and singlets respectively, we ignore the flavour indices for now, We assume that the EW phase transition is of the first order and that the bubble wall becomes relativistic, we will discuss later how to build such scenario. For the reasons that we will explain later, we need to assume that only the third generations couples to the heavy vector like B quark. Notice however that the interaction $LH\chi^c$ allowed by the gauge symmetries of the model but would violate the baryon number of one unit and lead to proton decay. We set it to zero in order to avoid this as this feature can be attributed to some accidental discrete symmetry. The baryon number are as follows: $B(\eta) = 2/3, B(\chi) = 1$, so that the m_χ violates the baryon symmetry by two units. The sweeping of the relativistic wall, via the collision of the b-quarks with bubbles, produces B_I, B_I^c and inside the bubble, we obtain the following abundances

$$n_{B_I} - n_{B_I^c} = -\theta_I^2 \epsilon_I n_b^0 \qquad\qquad n_b - n_{b^c} = \sum_I \theta_I^2 \epsilon_I n_b^0 \tag{42}$$

where n_b is the number density of the bottom-type quark, $\theta_I \approx \frac{Y_I \langle H \rangle}{M_I}$ is the mixing angle and ϵ_I is defined like in Eq. (26) (in this case there is no i index since we coupled it only to the third generation of quarks). The imaginary part of the loop function generated by a diagram similar to

12

the one of Fig.3 becomes

$$\text{Im}[f_B^{IJ}(x)] = \frac{1}{32\pi} \frac{M_I M_J}{M_I^2 - M_J^2} \frac{\sqrt{(M_I^2 - m_\eta^2 + m_\chi^2)^2 - 4m_\chi^2 M_I^2}}{M_I^4} \left(M_I^2 + m_\chi^2 - m_\eta^2\right) . \tag{43}$$

Like in the leptogenesis scenario, the asymmetry is separated in the heavy (B) and light b sector, with an opposite sign:

$$\sum_I \left(n_{B_I} - n_{B_I^c}\right) = -(n_b - n_{b^c}). \tag{44}$$

Let us see what will happen after B_I decays. If the mass spectrum satisfies $M_I > m_\chi > M_\eta$, there are four different channels, two leading to wash-outs and two enhancing the asymmetries:

(i) wash-out : $B_I \to \chi d^c u^c \to (bdud^c u^c)$ $B_I^c \to \chi^c du \to (b^c d^c u^c du)$

(ii) asymm. generation : $B_I \to \chi^c d^c u^c \to (b^c d^c u^c d^c u^c)$ $B_I^c \to \chi du \to (bdudu)$.

$$\tag{45}$$

As a result the asymmetry between SM quarks and antiquarks will be given

$$(n_q - n_{q^c}) = \sum_I (n_{B_I} - n_{B_I^c}) \left[\left(-\frac{5}{2} + \frac{1}{2}\right) Br(B_I \to \chi\eta^c) + Br(B_I \to bh)\right] + (n_b - n_{b^c})$$

$$, = -3 \sum_I (n_{B_I} - n_{B_I^c}) Br(B_I \to \chi\eta^c), \tag{46}$$

where we have used $Br(B_I \to \chi\eta^c) + Br(B_I \to bh) = 1$ and Eq.44 to derive the last relation. Finally, for the total baryon asymmetry we obtain

$$\frac{\Delta n_{Baryon}}{s} \approx \frac{135\zeta(3)}{8\pi^4} \sum_{I,J} \theta_I^2 \frac{|y_I|^2}{|y_I|^2 + |Y_I|^2} \times \frac{g_b}{g_\star} \left(\frac{T_{\text{nuc}}}{T_{\text{reh}}}\right)^3$$

$$\times \text{Im}(Y_I Y_J^* y_I^* y_J) \left(-\frac{2\text{Im}[f_B^{IJ}]}{|Y_I|^2} + \frac{4\text{Im}[f_B^{IJ}]|_{m_{\chi,\eta}\to 0}}{|y_I|^2}\right). \tag{47}$$

To match the observed baryon abundance, we need that

$$\Rightarrow \boxed{\theta_I^2 \left(\frac{T_{\text{nuc}}}{T_{\text{reh}}}\right)^3 \sim 10^{-(6-7)}}. \tag{48}$$

After this phase of fast decay, slow transition mediated by the heavy states can still wash out the asymmetry. They can be of two types:

- $b\eta \to \chi$: The Boltzmann equation controlling the interaction $b\eta \to \chi$ is

$$\frac{d\epsilon_q}{dz} = -\frac{0.42 e^{-z} z^{5/2}}{g_*^{1/2} g_q} \left(\frac{M_p}{m_\chi}\right) \left(\frac{g_\chi \Gamma(\chi \to \eta b)}{m_\chi}\right) \epsilon_q$$

$$\Gamma(\chi \to \eta b) \approx \left|\sum_I y_I \theta_I\right|^2 \frac{m_\chi (1 - m_\eta^2/m_\chi^2)}{8\pi g_\chi} \tag{49}$$

The requirement that this process is decoupled imposes a constraint on the mass of the field χ: $m_\chi/T_{\text{reh}} \gtrsim 30$. At the end of the day, the main constraint on the mass spectrum of our model is

$$\boxed{\frac{m_{B,\chi,\eta}}{T_{\text{reh}}} \gtrsim 30.} \tag{50}$$

This translates to bound $m_{B,\chi,\eta} \gtrsim 3$ TeV, or to a wall boost factor of the form

$$\frac{m^2_{B,\chi,\eta}}{T_{\text{nuc}}v} \gtrsim \gamma_w \tag{51}$$

or

$$\boxed{\gamma_w \gtrsim 10^3\,.} \tag{52}$$

Using Eq.(4), we observe that this corresponds to a supercooling

$$T_{\text{nuc}} \lesssim 10 \text{ GeV}\,. \tag{53}$$

- $ddu \leftrightarrow d^c d^c u^c$: Integrating out all the new heavy fields B, χ, η also generates new dangerous operators of the form

$$\frac{ddu\overline{d^c d^c u^c}}{M_\eta^4} \times \frac{1}{m_\chi} \times \theta^2 \qquad \Rightarrow \qquad \frac{1}{4\pi^5}\left(\frac{1}{16\pi^2}\right)^2 \frac{T_{\text{reh}}^{11}}{M_\eta^8 m_\chi^2}\theta^4 \lesssim \frac{T_{\text{reh}}^2}{M_p}. \tag{54}$$

However, this interaction, in all our parameter space, is always decoupled and do not bring any further wash out.

This low-energy model has the interesting consequence that it induces potential low-energy signatures. In this section, we enumerate those possible signatures without assuming that Q, u, and d are the third generation quarks.

$n - \bar{n}$ oscillations   Integrating out the heavy states, we obtain the following operator[53].

$$\frac{1}{\Lambda_{n\bar{n}}^5}\overline{u^c d^c d^c}udd \equiv \frac{(\sum \kappa\theta_I y_I)^2}{M_\eta^4 m_\chi}\overline{u^c d^c d^c}udd \quad \Rightarrow \quad \delta m_{\bar{n}-n} \sim \frac{\Lambda_{QCD}^6}{M_\eta^4 m_\chi}(\sum \kappa\theta_I y_I)^2. \tag{55}$$

Current bounds on this mixing mass are of order $\delta m_{\bar{n}-n} \lesssim 10^{-33}$ GeV [54–58]. It is very restrictive if B couples to light quarks, we conclude that we need to require that B only couples to the third family. Depending on the flavor of Q, u, d (the first or the third family) our scenario can be tested in the future experiment [59–62].

Flavor violation   For the η-diquark field that we used in this model, the FCNC are absent at tree level[63]. The loop level effects will however unavoidably lead to strong constraints if ηdu coupling contains the light generation quarks [63]. FCNC also forces B to couple mostly to the third family.

Bounds from EDMs   EDM are also typical signature of CP violation if it occurs at lowe energy

$$-i\frac{g_3\tilde{d}_q}{2}\bar{Q}\sigma^{\mu\nu}T^A\gamma_5 QG^A_{\mu\nu} \tag{56}$$

which is the chromo-electric dipole moment (see [64] for a review). The dipole in our model can be estimated to be

$$\frac{d_e}{e} \sim \frac{m_e(yYe)^2}{(4\pi)^6}\left(\frac{1}{\Lambda^2_{EDM}}\right) \sim 3\times 10^{-33}\times\left(\frac{10\text{TeV}}{\Lambda_{EDM}}\right)^2\text{cm} \tag{57}$$

which is much below the current experimental bound [65] $|d_e| < 1.1\times 10^{-29}\text{cm}\cdot e$.

So far we have left the phase transition sector inducing a fast wall for the EWPT undefined. The necessary ingredient for the mechanism is a strong first order electroweak phase transition and various studies indicate that even a singlet scalar (see ref.[66–72]) extensions of SM can help making the EWPT strongly first order. In [73], authors studied a singlet augmented SM in the case of a two steps phase transition. We study the following two steps PT

$$(0,0) \rightarrow (0,\langle s\rangle) \rightarrow (v_{EW},0)\ , \tag{58}$$

and focus on the region which induce relativistic bubbles. This pattern can occur if the m_s^2 parameter is positive. We will consider the following simple model

$$V_{\text{tree}}(H,s) = -\frac{m_h^2}{4}H^2 + \frac{m_H^2}{8v_{EW}^2}H^4 - \frac{m_s^2}{4}s^2 + \frac{\lambda_{hs}}{4}s^2H^2 + \frac{m_s^2}{8v_s^2}s^4\ . \tag{59}$$

where $v_{EW} = \sqrt{m_H^2/2\lambda}$ GeV and $v_s = \sqrt{m_s^2/2\lambda_s}$ correspond to the local minima at $(\langle H\rangle = v_{EW}, \langle s\rangle = 0)$ and $(\langle H\rangle = 0, \langle s\rangle = v_s)$ respectively. The origin of two-step PT can be intuitively understood from the following considerations. For simplicity let us ignore the Coleman-Weinberg potential and restrict the discussion by considering only the thermal masses. Then the potential will be given by

$$
\begin{aligned}
V(\mathcal{H},s) &\approx V_{\text{tree}}(\mathcal{H},s) + \frac{T^2}{24}\left[\sum_{bosons}n_iM_i^2(\mathcal{H},s)) + \frac{1}{2}\sum_{fermions}n_FM_F^2(\mathcal{H},s)\right], \\
&= V_{\text{tree}}(\mathcal{H},s) + T^2\left[h^2\left(\frac{g'^2}{32} + \frac{3g^2}{32} + \frac{m_h^2}{8v_{EW}^2} + \frac{y_t^2}{8} + \frac{\lambda_{hs}}{48}\right) + s^2\left(\frac{m_s^2}{16v_s^2} + \frac{\lambda_{hs}}{12}\right)\right].
\end{aligned}
\tag{60}
$$

From this expression we can clearly see that the temperatures when the minima with non zero vevs appear for the Higgs and singlet fields can be different. Then it can happen that the Z_2 breaking phase transition occurs before the EW one. This means that there will be first a phase transition from $(0,0) \rightarrow (0,v_s)$. We can now focus on the second PT, which is the real EWPT, $(0,v_s) \rightarrow (v_{EW},0)$. Due to a tuning of the term $-\frac{m_h^2}{4}H^2$ against $\frac{\lambda_{hs}}{4}v_s^2H^2$, the potential can become very flat around the false vacuum, leading to supercooling.

15
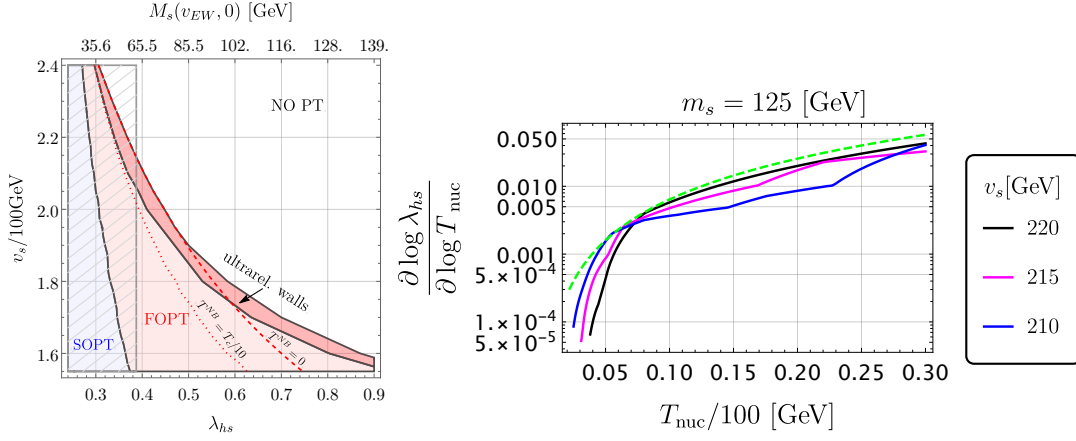
Figure 6: Left: scan of the parameter for the second PT. Right: Tuning of the coupling λ_{hs} as a function of the nucleation temperature. The dashed green line represents the naive tuning $\sim (T_{\text{nuc}}/m_h)^2$.

On Fig.6, we show the scan of the parameter of the second PT (Left) and the tuning required to obtain a given T_{nuc} (Right). We observe that having $T_{\text{nuc}} \sim 10$ GeV and leading to $\gamma_w \sim 10^3$ requires only moderate $\mathcal{O}(0.01)$ tuning.

An interesting follow-up would be to combine such scenario with the production of DM proposed in [35].

Acknowledgements

References

[1] **Planck** Collaboration, P. A. R. Ade et al. *Astron. Astrophys.* **594** (2016) A13, [arXiv:1502.01589].

[2] A. D. Sakharov *Pisma Zh. Eksp. Teor. Fiz.* **5** (1967) 32–35. [Usp. Fiz. Nauk161,no.5,61(1991)].

[3] A. Riotto, *Theories of baryogenesis*, in *ICTP Summer School in High-Energy Physics and Cosmology*, 7, 1998. hep-ph/9807454.

[4] D. Bodeker and W. Buchmuller arXiv:2009.07294.

[5] M. Fukugita and T. . Yanagida *Physics Letters B* **174** (1986), no. 1 45–47.

[6] V. Kuzmin, V. Rubakov, and M. Shaposhnikov *Phys. Lett. B* **155** (1985) 36.

[7] M. Shaposhnikov *JETP Lett.* **44** (1986) 465–468.

[8] A. E. Nelson, D. B. Kaplan, and A. G. Cohen *Nucl. Phys. B* **373** (1992) 453–478.

[9] M. Carena, M. Quiros, and C. E. M. Wagner *Phys. Lett. B* **380** (1996) 81–91, [hep-ph/9603420].

[10] J. M. Cline *Phil. Trans. Roy. Soc. Lond. A* **376** (2018), no. 2114 20170116, [arXiv:1704.08911].

[11] S. Bruggisser, B. Von Harling, O. Matsedonskyi, and G. Servant *JHEP* **12** (2018) 099, [arXiv:1804.07314].

[12] S. Bruggisser, B. Von Harling, O. Matsedonskyi, and G. Servant *Phys. Rev. Lett.* **121** (2018), no. 13 131801, [arXiv:1803.08546].

[13] D. E. Morrissey and M. J. Ramsey-Musolf *New J. Phys.* **14** (2012) 125003, [arXiv:1206.2942].

[14] C. Caprini and J. M. No *JCAP* **01** (2012) 031, [arXiv:1111.1726].

[15] J. M. Cline and K. Kainulainen *Phys. Rev. D* **101** (2020), no. 6 063525, [arXiv:2001.00568].

[16] G. C. Dorsch, S. J. Huber, and T. Konstandin arXiv:2106.06547.

[17] B. Shuve and C. Tamarit *JHEP* **10** (2017) 122, [arXiv:1704.01979].

[18] I. Baldes, S. Blasi, A. Mariotti, A. Sevrin, and K. Turbang arXiv:2106.15602.

[19] A. Azatov and M. Vanvlasselaer *JCAP* **01** (2021) 058, [arXiv:2010.02590].

[20] W.-Y. Ai, B. Laurent, and J. van de Vis *JCAP* **07** (2023) 002, [arXiv:2303.10171].

[21] W.-Y. Ai, X. Nagels, and M. Vanvlasselaer arXiv:2401.05911.

[22] D. Bodeker and G. D. Moore *JCAP* **0905** (2009) 009, [arXiv:0903.4099].

[23] D. Bodeker and G. D. Moore *JCAP* **1705** (2017), no. 05 025, [arXiv:1703.08215].

[24] Y. Gouttenoire, R. Jinno, and F. Sala *JHEP* **05** (2022) 004, [arXiv:2112.07686].

[25] A. Azatov, G. Barni, R. Petrossian-Byrne, and M. Vanvlasselaer arXiv:2310.06972.

[26] E. J. Chun, T. P. Dutka, T. H. Jung, X. Nagels, and M. Vanvlasselaer *JHEP* **09** (2023) 164, [arXiv:2305.10759].

[27] A. Azatov, M. Vanvlasselaer, and W. Yin *JHEP* **10** (2021) 043, [arXiv:2106.14913].

[28] M. Fukugita and T. Yanagida *Phys. Lett. B* **174** (1986) 45–47.

[29] J. A. Harvey and M. S. Turner *Phys. Rev. D* **42** (1990) 3344–3349.

[30] P. Minkowski *Phys. Lett. B* **67** (1977) 421–428.

[31] T. Yanagida *Conf. Proc. C* **7902131** (1979) 95–99.

[32] M. Gell-Mann, P. Ramond, and R. Slansky *Conf. Proc. C* **790927** (1979) 315–321, [arXiv:1306.4669].

[33] S. L. Glashow *NATO Sci. Ser. B* **61** (1980) 687.

[34] R. N. Mohapatra and G. Senjanovic *Phys. Rev. Lett.* **44** (1980) 912.

[35] A. Azatov, M. Vanvlasselaer, and W. Yin *JHEP* **03** (2021) 288, [arXiv:2101.05721].

[36] B. Laurent and J. M. Cline *Phys. Rev. D* **102** (2020), no. 6 063516, [arXiv:2007.10935].

[37] C. Caprini et al. arXiv:1910.13125.

[38] D. J. Weir *Phil. Trans. Roy. Soc. Lond. A* **376** (2018), no. 2114 20170126, [arXiv:1705.01783].

[39] P. Amaro-Seoane, H. Audley, S. Babak, J. Baker, E. Barausse, P. Bender, E. Berti, P. Binetruy, M. Born, D. Bortoluzzi, J. Camp, C. Caprini, V. Cardoso, M. Colpi, J. Conklin, N. Cornish, C. Cutler, K. Danzmann, R. Dolesi, L. Ferraioli, V. Ferroni, E. Fitzsimons, J. Gair, L. G. Bote, D. Giardini, F. Gibert, C. Grimani, H. Halloin, G. Heinzel, T. Hertog, M. Hewitson, K. Holley-Bockelmann, D. Hollington, M. Hueller, H. Inchauspe, P. Jetzer, N. Karnesis, C. Killow, A. Klein, B. Klipstein, N. Korsakova, S. L. Larson, J. Livas, I. Lloro, N. Man, D. Mance, J. Martino, I. Mateos, K. McKenzie, S. T. McWilliams, C. Miller, G. Mueller, G. Nardini, G. Nelemans, M. Nofrarias, A. Petiteau, P. Pivato, E. Plagnol, E. Porter, J. Reiche, D. Robertson, N. Robertson, E. Rossi, G. Russano, B. Schutz, A. Sesana, D. Shoemaker, J. Slutsky, C. F. Sopuerta, T. Sumner, N. Tamanini, I. Thorpe, M. Troebs, M. Vallisneri, A. Vecchio, D. Vetrugno, S. Vitale, M. Volonteri, G. Wanner, H. Ward, P. Wass, W. Weber, J. Ziemer, and P. Zweifel, *Laser interferometer space antenna*, 2017.

[40] C. Caprini et al. *JCAP* **1604** (2016), no. 04 001, [arXiv:1512.06239].

[41] B. Von Harling, A. Pomarol, O. Pujolàs, and F. Rompineve *JHEP* **04** (2020) 195, [arXiv:1912.07587].

[42] V. Brdar, A. J. Helmboldt, and J. Kubo *JCAP* **02** (2019) 021, [arXiv:1810.12306].

[43] V. Corbin and N. J. Cornish *Class. Quant. Grav.* **23** (2006) 2435–2446, [gr-qc/0512039].

[44] J. Crowder and N. J. Cornish *Phys. Rev. D* **72** (2005) 083005, [gr-qc/0506015].

[45] N. Seto, S. Kawamura, and T. Nakamura *Phys. Rev. Lett.* **87** (2001) 221103, [astro-ph/0108011].

[46] K. Yagi and N. Seto *Phys. Rev. D* **83** (2011) 044011, [arXiv:1101.3940]. [Erratum: Phys.Rev.D 95, 109901 (2017)].

[47] S. Isoyama, H. Nakano, and T. Nakamura *PTEP* **2018** (2018), no. 7 073E01, [arXiv:1802.06977].

[48] S. Hild et al. *Class. Quant. Grav.* **28** (2011) 094013, [arXiv:1012.0908].

[49] B. Sathyaprakash et al. *Class. Quant. Grav.* **29** (2012) 124013, [arXiv:1206.0331]. [Erratum: Class. Quant. Grav.30,079501(2013)].

[50] M. Maggiore et al. *JCAP* **03** (2020) 050, [arXiv:1912.02622].

[51] L. Badurina et al. *JCAP* **05** (2020) 011, [arXiv:1911.11755].

[52] **AEDGE** Collaboration, Y. A. El-Neaj et al. *EPJ Quant. Technol.* **7** (2020) 6, [arXiv:1908.00802].

[53] K. Fridell, J. Harz, and C. Hati arXiv:2105.06487.

[54] M. Baldo-Ceolin et al. *Z. Phys. C* **63** (1994) 409–416.

[55] **Super-Kamiokande** Collaboration, K. Abe et al. *Phys. Rev. D* **91** (2015) 072006, [arXiv:1109.4227].

[56] S. Rao and R. Shrock *Phys. Lett. B* **116** (1982) 238–242.

[57] M. I. Buchoff, C. Schroeder, and J. Wasem *PoS* **LATTICE2012** (2012) 128, [arXiv:1207.3832].

[58] S. Syritsyn, M. I. Buchoff, C. Schroeder, and J. Wasem *PoS* **LATTICE2015** (2016) 132.

[59] D. G. Phillips, II et al. *Phys. Rept.* **612** (2016) 1–45, [arXiv:1410.1100].

[60] D. Milstead *PoS* **EPS-HEP2015** (2015) 603, [arXiv:1510.01569].

[61] **NNbar** Collaboration, M. J. Frost, *The NNbar Experiment at the European Spallation Source*, in *7th Meeting on CPT and Lorentz Symmetry*, 7, 2016. arXiv:1607.07271.

[62] J. E. T. Hewes, *Searches for Bound Neutron-Antineutron Oscillation in Liquid Argon Time Projection Chambers.* PhD thesis, Manchester U., 2017.

[63] G. F. Giudice, B. Gripaios, and R. Sundrum *JHEP* **08** (2011) 055, [arXiv:1105.3161].

[64] J. Engel, M. J. Ramsey-Musolf, and U. van Kolck *Prog. Part. Nucl. Phys.* **71** (2013) 21–74, [arXiv:1303.2371].

[65] **ACME** Collaboration, V. Andreev et al. *Nature* **562** (2018), no. 7727 355–360.

[66] G. W. Anderson and L. J. Hall *Phys. Rev. D* **45** (Apr, 1992) 2685–2698.

[67] J. Choi and R. R. Volkas *Phys. Lett. B* **317** (1993) 385–391, [hep-ph/9308234].

[68] J. R. Espinosa and M. Quiros *Phys. Lett. B* **305** (1993) 98–105, [hep-ph/9301285].

[69] S. Profumo, M. J. Ramsey-Musolf, and G. Shaughnessy *JHEP* **08** (2007) 010, [arXiv:0705.2425].

[70] J. R. Espinosa, T. Konstandin, and F. Riva *Nucl. Phys. B* **854** (2012) 592–630, [arXiv:1107.5441].

[71] C.-Y. Chen, J. Kozaczuk, and I. M. Lewis *JHEP* **08** (2017) 096, [arXiv:1704.05844].

[72] J. Ellis, M. Lewicki, and J. M. No *JCAP* **04** (2019) 003, [arXiv:1809.08242].

[73] A. Azatov, G. Barni, S. Chakraborty, M. Vanvlasselaer, and W. Yin *JHEP* **10** (2022) 017, [arXiv:2207.02230].